Inner reorganization during the radical–biradical transition in a nor-β-lapachone derivative possessing two redox centers†

Dulce María Hernández,[a] Maria Aline B. F. de Moura,[b] Drochss Pettry Valencia,[a] Felipe J. González,[a] Ignacio González,[c] Fabiane C. de Abreu,[b] Eufrânio N. da Silva Júnior,[d] Vitor F. Ferreira,[d] Antônio Ventura Pinto,[e] Marilia O. F. Goulart*[b] and Carlos Frontana*[a]

Received 14th April 2008, Accepted 10th June 2008
First published as an Advance Article on the web 16th July 2008
DOI: 10.1039/b806271d

In this work, the electrochemical behaviour of an antitumoral nitro o-quinone derivative obtained from 3-bromo-nor-β-lapachone was studied. Cyclic voltammetric experiments, in acetonitrile solution, revealed that both quinone and nitro functions are reduced independently as *quasi*-reversible one-electron transfer processes in this order. Depending on the reduction potential, a radical anion or a biradical dianion is obtained. The formation of these paramagnetic species was confirmed by performing *in situ* Electrochemical-Electron Spin Resonance (E-ESR) experiments. Analysis of the kinetics of electron transfer associated to those electron uptake processes, in terms of the Marcus–Hush–Levich model, revealed differences in the reorganization energy ($\lambda^{(k)}$) for both steps ($\lambda^{(I)}$: 1.07–1.11 eV; $\lambda^{(II)}$: 1.21–1.30 eV). By evaluating the conformations of the radical and biradical systems by calculations at the BLYP//TZVP level of theory, it was found that the inner component, for the second reduction process ($\lambda^{(II)}$) was approximately 72% of $\lambda^{(II)}$, reflecting modifications in the molecular structure during the radical anion–biradical dianion transition. This change is also reflected in the differences presented by line widths of the ESR signals of both electrogenerated radical and diradical species.

1. Introduction

Quinones play a major role as bioreductive drugs, oxidative stress enhancers, and redox catalysts.[1–8] As Michael acceptors, quinones can induce cellular damage through alkylation of crucial cellular proteins and/or DNA. Alternatively, they are highly redox active molecules which can, by intermediacy of their semiquinone radicals or hydroquinones, lead to formation of reactive oxygen species (ROS). These species cause severe oxidative stress within cells through the formation of oxidized cellular macromolecules, including lipids, proteins, and DNA. ROS can also activate a number of signaling pathways.[8] Additionally, quinones can work as DNA intercalators, inhibitors of topoisomerases and of some enzymes of the mitochondrial electron transfer chain.[2–6] The striking feature of quinone chemistry is the ease of reduction and therefore the ability of quinones to act as oxidizing or dehydrogenating agents. The driving force for such a facilitated reaction is the formation, after reduction, of a fully aromatic ring.[7–10]

The toxicology of quinones is modulated by the presence of substituents that effectively determine the relative participation of their oxidant and electrophilic properties. For instance, the presence of an electron-withdrawing group confers stronger oxidant properties on the quinone, but the corresponding hydroquinone or catechol is less readily oxidized. Conversely, with electron-donating substitution, the oxidant power is less pronounced, but the corresponding hydroquinone or catechol is more easily oxidized. The electrochemical properties of the quinone compounds are very important for their bioreductive activation, either to the semiquinone or to the hydroquinone. Concerning nitrocompounds, their assumed biological activity is also related to their facile reduction to $RNO_2^{\bullet -}$ species, promoted *in vivo* by nitroreductases.[7,11,12]

Nitroquinones have been investigated with special toxicological concern. Electroreduction of nitro derivatives of quinones has been described,[13–18] but, in the majority of cases, without considering any relationship with pharmacological activities and any evidence of mechanistic complications, as demonstrated in the case of 2-nitronaphthothiophen-4,9-quinone,[19] which carries two different electrochemically reducible sites and presents a conjugate interaction.

2,2-Dimethyl-3-(3-nitro-phenylamino)-2,3-dihydronaphtho[1,2-*b*]furan-4,5-dione (**1**) (Scheme 1), a nor-β-lapachone derivative, also carries two pharmacophoric and electroactive groups, the quinone and the nitroaromatic moieties, in non-conjugated

[a]*Departamento de Química, Centro de Investigación y Estudios Avanzados, Av. Instituto Politécnico Nacional No. 2508, San Pedro Zacatenco, C. P. 07360, México. E-mail: ultrabuho@yahoo.com.mx*
[b]*Instituto de Química e Biotecnologia, Universidade Federal de Alagoas, Tabuleiro do Martins, Maceió, Alagoas, 57072-970, Brazil. E-mail: mofg@qui.ufal.br*
[c]*UAM-Iztapalapa, Depto. de Química, Área de Electroquímica, Apartado Postal 55-534, 09340, México*
[d]*Instituto de Química, Universidade Federal Fluminense, Campus Valonguinho, Niterói, CEP 24020-150, Brazil*
[e]*Núcleo de Pesquisa em Produtos Naturais, NPPN, Universidade Federal do Rio de Janeiro, 21944-971, Rio de Janeiro, RJ, Brazil*

† Electronic supplementary information (ESI) available: Geometric parameters (bond distances and angles) as obtained from electronic structure calculations at the BLYP/TZVP level of theory for the neutral, radical anion and biradical dianion structures for the studied compound. See DOI: 10.1039/b806271d

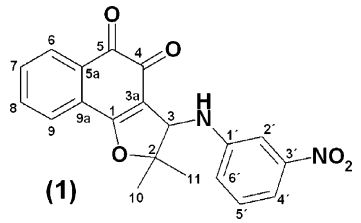

Scheme 1

environments.[20] Its cytotoxic activity against several cancer lines was reported,[20] showing potent cytotoxicity against six neoplastic cancer cells: SF-295 (central nervous system, 1.37 μM), HCT-8 (colon, 1.76 μM), MDAMB-435 (melanoma, 0.63 μM), HL-60 (leukaemia, 0.91 μM), PC-3 (prostate, 1.12 μM), and B-16 (murine melanoma, 1.18 μM), despite absence of selectivity.[20]

As the electrophilic character of quinones has been proved to be relevant for several biological activities[7,8,18,21] and considering that the presence of a nitro substituent certainly makes the electron capture by the quinone moiety easier, this paper intends to consider the mutual influence of the redox groups on the electron transfer processes of **1** and the structural properties of the radical anions electrochemically generated.

2. Experimental

Cyclic voltammetry experiments were performed using a PG-STAT 100 AUTOLAB electrochemical analyzer interfaced with a personal computer. Cyclic voltammetry experiments at several scan rates within the interval: $0.1 \leq v \leq 10$ Vs^{-1}, were performed, applying IR drop compensation with R_u values determined from positive feedback measurements (R_u: 154 Ω).[22,23] This value leads to a variation lower than 1.5 mV dec^{-1} for the anodic peak potential of ferrocene and for the cathodic peak potential of anthracene (from 0.01 to 10 V s^{-1}). A glassy carbon disk electrode (0.07 cm^2) was used as a working electrode, polished with 0.05 μm alumina powder (Buehler), and rinsed with acetone before each voltammetric run. A platinum wire and a commercial saturated calomel electrode (SCE), this last being separated from the medium with a salt bridge filled with the supporting electrolyte solution, were used as the auxiliary and reference electrodes, respectively. The potential values obtained are referred to the ferrocenium/ferrocene (Fc^+/Fc) couple, as recommended by IUPAC.[24] The potential for this redox couple, determined from voltammetric studies, was 0.41 V *vs.* SCE. The studies were carried out in an inert atmosphere by saturation with high purity argon (Praxair grade 5.0) at room temperature (~22 °C).

2,2-Dimethyl-3-(3-nitro-phenylamino)-2,3-dihydronaphtho[1,2-*b*]furan-4,5-dione (**1**) was synthesized according to a procedure described earlier.[21] Acetonitrile (CH_3CN), Merck® spectroscopic grade, distilled from P_2O_5 and kept under molecular sieves (3 Å, Merck®) was used as solvent. Tetrabutylammonium hexafluorophosphate (n-Bu_4NPF_6, Aldrich®), recrystallized from hexane–ethyl acetate mixtures, was used as supporting electrolyte. All the solutions were purged with high purity argon (Praxair, Grade 5.0) for 25 minutes before each series of experiments.

ESR spectra were recorded in the X band (9.85 GHz), using a Brucker ELEXSYS 500 instrument with a rectangular TE_{102} cavity. A commercially available spectroelectrochemical cell (Wilmad) was used. A platinum mesh (~0.2 cm^2) was introduced in the flat path of the cell and used as a working electrode. Another platinum wire was used as a counter electrode (2.5 cm^2). Ag/0.01 mol L^{-1} $AgNO_3$ + 0.1 mol L^{-1} tetrabutylammonium perchlorate reference in acetonitrile (BAS) was employed as the reference electrode. Potential control was performed with a 263 Princeton Applied Research potentiostat/galvanostat. The employed solutions were prepared in the same fashion as the ones used for the electrochemical studies. PEST WinSim free software, version 0.96 (National Institute of Environmental Health Sciences), was used to perform ESR spectra simulation, from the hyperfine coupling constant values (HFCC, *a*) measured, to compare with the experimental ones. This program was also used to evaluate *a* values in the case when a direct measurement would be difficult under the spectra acquisition conditions.

3. Calculations

Electronic structure calculations were performed using the DeMon2k code[25] using the TZVP basis set[26,27] and the functional of Lee, Yang and Parr[28,29] to account for electronic correlation. Full geometry optimization was performed (no geometry constrains) for the neutral, radical and biradical structures experimentally detected, employing RHF and UHF (restricted and unrestricted Hartree–Fock) calculations as required. Vibrational analysis was performed to check that the obtained structures were indeed the minimum energy conformers, characterized by the lack of negative vibrational frequencies. These structures were used as inputs for single point energy calculations at the same theory level. From this data, spin density values were evaluated as the difference between α and β spin densities (from s type orbitals in the case of H atoms and from the mean value obtained from p_x, p_y and p_z orbitals for N atoms).[30]

4. Results and discussion

4.1. Electrochemical characterization

Cyclic voltammograms for a solution of **1** were obtained in the potential region between the open circuit potential (−0.26) and −2.7 V *vs.* Fc^+/Fc (Fig. 1).

From the obtained voltammograms, three main reduction signals [Ic ($Ep_{Ic} = -1.15$ V *vs.* Fc^+/Fc), IIc ($Ep_{IIc} = -1.66$ V *vs.* Fc^+/Fc) and IIIc ($Ep_{IIIc} = -2.33$ V *vs.* Fc^+/Fc)] can be observed. At the scan rate employed, the first one (Ic) is associated to oxidation signal Ia in a *quasi*-reversible process ($Ep_{Ia} - Ep_{Ic} = 71$ mV), and the second one corresponds to another *quasi*-reversible couple consisting of signals IIc and IIa ($Ep_{IIa} - Ep_{IIc} = 81$ mV). However, peak IIIc shows a chemically irreversible behavior, characterized by the presence of the anodic peak (IIIa), which appears at potential values between peaks Ia and IIa. The intensity of this signal increases by setting increasingly more negative potential values at the inversion of the scan direction.

Considering the fact that reduction of nitro compounds could occur at potential values in the region where signal IIc appears,[11,19,31] the structural nature of the radical anion formed in the first electron transfer step is difficult to establish directly, as it occurs for single quinones or nitrocompounds. Representing compound **1** as [Q]-$PhNO_2$, this species could be either [$Q^{\bullet -}$]-$PhNO_2$ or

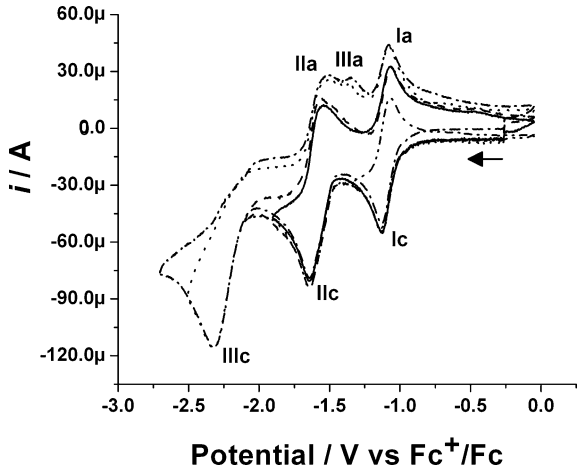

Fig. 1 Cyclic voltammograms of 1.2×10^{-3} mol L^{-1} **1** in 0.1 mol L^{-1} *n*-Bu_4NPF_6–CH_3CN. Voltammograms at different inversion potential conditions are shown. *v*: 100 mV s^{-1}. WE: glassy carbon (0.07 cm^2).

[Q]-$PhNO_2^{\bullet -}$. Consequently, and in order to discriminate between both possibilities, ESR-electrochemical experiments were carried out.

4.2. ESR spectro-electrochemical characterization

Upon reduction of a 1.2 mM solution of compound **1**, at a constant potential between peaks Ic and IIc, an *in situ* ESR spectral structure was detected (Fig. 2).

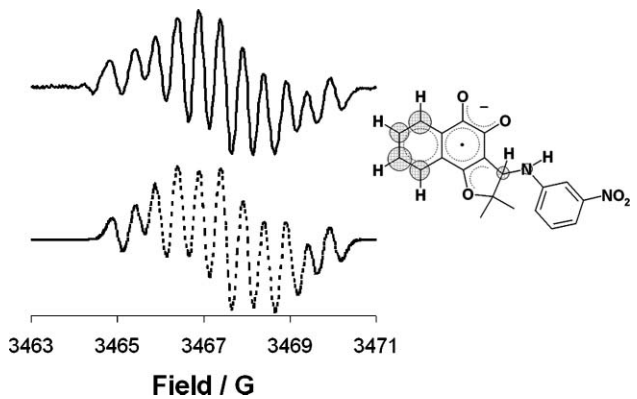

Fig. 2 ESR spectra for the electrogenerated radical species of 1.2×10^{-3} mol L^{-1} **1** in 0.1 mol l^{-1} *n*-But_4NBF_4–CH_3CN at $E_{appl} = -1.25$ V *vs.* Fc^+/Fc. Modulation amplitude: 0.05 G. The solid upper line indicates the experimental spectrum, while the dotted lower line indicates simulated spectra from calculated HFCC values. The spin density structure evaluated from the analysis of the experimental data is shown in the figure.

The ESR spectrum observed consists of 6 different hyperfine coupling constant values (HFCC) (Table 1), all assigned to the interaction between the nuclear spin of H atoms with the unpaired electron of the electrogenerated radical anion. Considering the number of these interactions, the observed radical structure is related to the generation of the semiquinone radical upon reduction of the *o*-quinone functionality at positions C-4 and C-5. This result indicates that signals Ic-Ia are related to the redox reaction depicted by eqn (1), which is consistent with the proposal presented earlier for the reduction of this type of compound bearing both a nitro and an *o*-quinone function in the same molecule.[19]

$$[Q]\text{-}PhNO_2 + e^- \rightleftharpoons [Q^{\bullet -}]\text{-}PhNO_2 \quad (1)$$

Still, as already depicted, the nature of the second reduction step is more difficult to discern, as in the molecule there are two remaining groups capable of being reduced: the generated semiquinone from the previous electrochemical uptake,[19] or the nitroaromatic group at position C-3′. This competition is interesting, as in the former case (eqn (2a)), the system would behave as a typical two consecutive one-electron reduction process of quinones in aprotic media affording a quinone dianion $[Q^{2-}]$-$PhNO_2$[32–34] but in the latter (eqn (2b)), it would be possible to generate another independent radical species, associated to the nitro radical anion [Q•−]-$PhNO_2^{\bullet -}$.[19]

$$[Q^{\bullet -}]\text{-}PhNO_2 + e^- \rightleftharpoons [Q^{2-}]\text{-}PhNO_2 \quad (2a)$$

$$[Q^{\bullet -}]\text{-}PhNO_2 + e^- \rightleftharpoons [Q^{\bullet -}]\text{-}PhNO_2^{\bullet -} \quad (2b)$$

In order to discriminate the nature of both independent electron transfer steps, the spectroelectrochemical-electron spin resonance (ESR) was also performed to analyze the nature of the electrogenerated products from reduction process IIc. Upon setting the applied potential at values near the potential region of signal IIc, a second radical structure appears (Fig. 3A) besides that observed in Fig. 2.

The observed spectrum indicates the presence of a second radical structure (Fig. 3B), which presents a larger HFCC value associated to the interaction of the unpaired electron with an N atom from a nitro functionality (Table 1).[35] Another set of HFCC values are also obtained, arising from the interaction of this unpaired electron with the H atoms present in the aromatic ring that bears the NO_2 group (C-2′, C-4′, C-5′ and C-6′, Table 1). Therefore, the second reduction process observed experimentally is assigned to the reduction of the nitro function (eqn (2b)), thus leading to the formation of a stable biradical dianion structure at potential values higher than peak IIc (Fig. 3C), the spin density of which is represented in Fig. 4.

Interestingly, no decrease of the intensity of the first radical observed experimentally was detected and therefore, the reduction

Table 1 Hyperfine coupling constants and linewidths for the electrogenerated radical anion structures for compound **1**[a]

Radical structures	a_1/G	a_2/G	a_3/G	a_4/G	a_5/G	a_6/G	Γ/G	g
First radical anion[b]	0.59 (H-3)	0.9 (H-6)	1.1 (H-7)	0.89 (H-8)	1.04 (H-9)	0.48 (NH)	0.32	2.0029
Second radical anion[c]	3.46 (H-2′)	3.02 (H-4′)	1.03 (H-5′)	3.43 (H-6′)	10.93 (N-3′)	NA	0.16	2.0032

[a] Assignments for each hyperfine coupling constant with the corresponding hydrogen atom are indicated for each signal (see Fig. 1 for numbering). [b] Radical obtained upon reduction at $E_{appl} = -1.25$ V *vs.* Fc^+/Fc. [c] Radical obtained upon reduction at $E_{appl} = -1.80$ V *vs.* Fc^+/Fc. NA: not applicable.

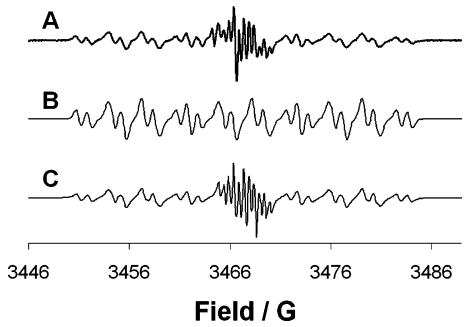

Fig. 3 ESR spectra for the electrogenerated radical species of 1.2×10^{-3} mol L^{-1} **1** in 0.1 mol l^{-1} *n*-But_4NBF_4–CH_3CN at $E_{appl} = -1.80$ V *vs.* Fc^+/Fc. Modulation amplitude: 0.05 G. (A) Experimental spectrum, (B) simulated second radical structure from spectrum A, as obtained from HFCC values, (C) simulated mixture of structures of the radical anions from Fig. 4 and spectrum B.

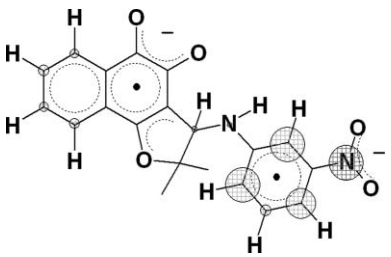

Fig. 4 Spin density structure of the biradical dianion electrogenerated at $E_{appl} = -1.80$ V *vs.* Fc^+/Fc as evaluated from the analysis of the experimental data. Spin densities were re-sized to reflect the relative magnitude of each experimental HFCC value.

of the semiquinone structure into the quinone dianion species does not occur at potential values near peak IIc. This suggests that the stability of the biradical dianion structure detected experimentally shifts the reduction potential value of the semiquinone/quinone dianion formation to more negative potentials. However, upon *in situ* reduction of species $[Q^{\bullet -}]$-$PhNO_2^{\bullet -}$ at potential values near peak IIIc ($Ep_{IIIc} = -2.5$ V *vs.* Fc^+/Fc), the second radical structure experimentally observed (Fig. 3B) begins to disappear, leading us to only register again the semiquinone radical alone in solution. This indicates that upon reduction at peak IIIc, the nitro radical anion moiety transforms into a dianion structure $[Q^{\bullet -}]$-$PhNO_2^{2-}$, which undergoes a fast chemical process, in agreement with the chemically irreversible character of signal IIIc. This chemical process is proposed to be related to the formation of the hydroxylamine, involving the uptake of three more electrons by the nitro radical anion structure. The electrogenerated hydroxylamine is oxidized at the level of signal IIIa.[36] In this work, the processes associated to peak IIIc will not be discussed further.

Linewidths (Γ) of both electrogenerated radicals indicate differences in relaxation times for both participating species.[30] For the semiquinone radical anion, Γ attains a larger value (0.32 G), than for the nitro radical anion (0.16 G, Table 1). This indicates that spin exchange or homogeneous electron transfer between the semiquinone radical anion fragment and neutral structures[30] occurs at a faster rate than for the nitro radical anion fragment. As the nature of these relaxation phenomena is strongly related to the rate of electron transfer of the given structure, with broader linewidths being related to faster electron exchange processes and *vice versa*, these results confirm the difference in reorganization energies found experimentally for the formation of both radical species. We can deduce from the observations above that the semiquinone radical anion would present a higher value for the rate constant of electron transfer than the nitro radical anion, as will be evaluated later.

4.3. Experimental evaluation of the reorganization energy (λ)

Considering the reversible and quasireversible behavior observed (Fig. 1) for the first (Ic/Ia) and second (IIc/IIa) reduction processes, an electrochemical analysis was performed by evaluating the separation in potential between the corresponding reduction and oxidation peaks ($\Delta E_{pIc\text{-}Ia}$; $\Delta E_{pIIc\text{-}IIa}$) as a function of the scan rate (Fig. 5). From this approach, the standard heterogeneous rate constants of electron transfer $k^{0(I)}$ and $k^{0(II)}$ could be determined using the methodology described by Nicholson.[37] However, in this model it appears as if both $k°$ and a were independent parameters, considering the Butler–Volmer formalism,[38,39] and therefore it is required to overrun this disadvantage. An alternative way of dealing with this problem was carried out by simulating the variations of $\Delta E_{pIc\text{-}Ia}$ and $\Delta E_{pIIc\text{-}IIa}$ in terms of the respective reorganization energies $\lambda^{(I)}$, and $\lambda^{(II)}$, as occurs within the framework of the Marcus–Hush–Levich theory.[40–43] For this purpose, a number of values for $\lambda^{(k)}$, covering the transition between fast and slow electron transfer behavior, were chosen (0.7 to 1.4 eV), as had been tested earlier for analyzing the reduction of quinones in acetonitrile.[44] With these energy values, $k^{0(I)}$ and $k^{0(II)}$ can be calculated employing eqn (3),

$$k^{0(I\,or\,II)} = A \exp\left(\frac{-\Delta G^{\ddagger}_{I\,or\,II}}{RT}\right) \tag{3}$$

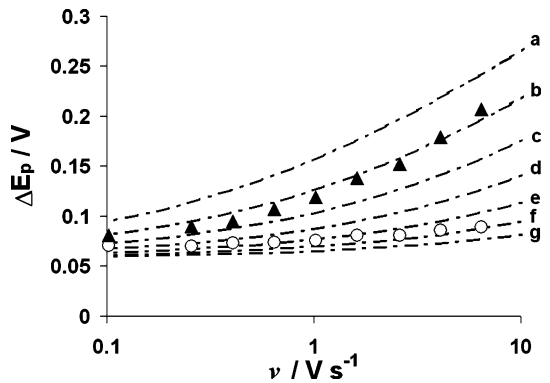

Fig. 5 Variations of the experimental ΔE_p for the first (○) and second (▲) reduction processes for **1** as a function of the scan rate. Dotted lines depict the calculated $\Delta E_{pIc\text{-}Ia}$ variations at different reorganization energies (D_{model}: 2×10^{-5} cm^2). λ values plotted: (a) 1.31; (b) 1.26; (c) 1.21; (d) 1.16; (e) 1.12; (f) 1.07; (g) 1.02 eV.

considering

$$\Delta G^{\ddagger}_{(I\text{ or }II)} = \lambda/4 \tag{4}$$

The pre-exponential factor A can be estimated as the average value of the component of velocity in the direction of the electrode[40]

$$A = (RT/2\pi M)^{1/2} \tag{5}$$

For the molecule studied, A was set as 5.5×10^3 cm s^{-1}. Both $\lambda^{(\mathrm{I\ or\ II})}$ and $k^{0(\mathrm{I\ or\ II})}$, as well as the diffusion coefficient of the molecule ($D = 1.95 \pm 0.12 \times 10^{-5}$ cm^2 s^{-1}) were inputted in a digital simulation program (Digielch 4.0®)[45–50] to obtain simulated cyclic voltammograms. From these voltammograms, variations of both $\Delta E_{\mathrm{pIc\text{-}Ia}}$ and $\Delta E_{\mathrm{pIIc\text{-}IIa}}$ values as a function of the reorganization energy were obtained (Fig. 5). The diffusion coefficient was evaluated by performing a potential step under Cottrell conditions (between peaks Ic and IIc) and from the intercept of a plot of $I \cdot t^{1/2}$ *vs.* $t^{1/2}$, at times closer to 3 seconds, long enough to ensure diffusion limited processes without involving convection.[51]

Experimental data obtained for compound **1** presented a fair fit with the calculated curves (Fig. 5). The obtained values for the reorganization energy for each signal ($\lambda^{(\mathrm{I})}$ and $\lambda^{(\mathrm{II})}$) indicate a significant difference in rates for the observed processes, the first one being faster ($1.07 < \lambda^{(\mathrm{I})} < 1.11$ eV), than the second ($1.21 < \lambda^{(\mathrm{II})} < 1.3$ eV). The difference between both λ values indicates also that the uptake of the first electron by the molecule influences the nuclear reorganization energy required during the second electron transfer step.

4.4. Contributions of outer and inner reorganization components during the reduction processes

The chemical mechanism by which the structure presents these differences in terms of rates of electron transfer remains to be addressed. For this purpose, calculations were performed to evaluate the influence of the inner [$\lambda_i^{(\mathrm{I\ or\ II})}$] and outer [$\lambda_o^{(\mathrm{I\ or\ II})}$] components of the reorganization energy (λ) for compound **1**. Typically, λ_o components are regarded as having the most influence in the total reorganization energy λ. These components can be calculated by assuming a hard sphere solvation model considering image force effects on the electrode,[42,52–54]

$$\lambda_o = \frac{N_A e^2}{8\pi\varepsilon_0}\left(\frac{1}{a_{Ox}} - \frac{1}{r}\right)\left(\frac{1}{\varepsilon_{op}} - \frac{1}{\varepsilon_S}\right) \tag{6}$$

where N_A is Avogadro's number, e is the charge of an electron, ε_0 is the permittivity of vacuum, a_{Ox} is the radius of the molecule under electron transfer and r is the distance between the molecule and the electrode surface, assumed as having an infinite value for a pure outer sphere electron transfer process. ε_{op} and ε_S are the optical and static dielectric constants of the medium, the first being considered as the inverse of the square for the refractive index and the second as the inverse of the dielectric constant both for pure acetonitrile.[55,56] $a_{Ox} = 10.8$ Å was evaluated from D, as the hydrodynamic radius of the molecule, considering the Stokes–Einstein relationship[57]

$$a_{Ox} = \frac{\kappa_B T}{6\pi\eta D_{Ox}} \tag{7}$$

where κ_B is the Boltzmann constant, T is the absolute temperature, η is the viscosity of the medium employed (approx. 0.00104 g cm^{-1} s^{-1})[58] and D_{Ox} is the experimental diffusion coefficient of the species being reduced. Considering the experimental data presented in this work, $\lambda_o^{(\mathrm{I\ or\ II})}$ attains a value of nearly 0.35 eV. It should be noted that this value would be the same for both reduction processes being considered ($\lambda_o^{(\mathrm{I})} = \lambda_o^{(\mathrm{II})}$), as long as D does not change significantly (slight changes in molecular volume‡)[59] from the first electron uptake to the second.

The results of $\lambda_o^{(\mathrm{I})}$ and $\lambda_o^{(\mathrm{II})}$ account only partially for the total values of $\lambda^{(\mathrm{I})}$ (~32%) and $\lambda^{(\mathrm{II})}$ (~28%) obtained experimentally, and indicate that the inner components of $\lambda_i^{(\mathrm{I})}$ and $\lambda_i^{(\mathrm{II})}$ have a more significant contribution. An estimate of the inner reorganization energy can be calculated using a rather simple approach presented earlier by Nelsen *et al.*,[60] evaluating $\lambda_i^{(\mathrm{I\ or\ II})}$ from the difference in energy of the electron self-exchange reaction $\lambda_{i,\mathrm{exch}}^{(\mathrm{I\ or\ II})}$. This is possible as, in this type of reaction, the nuclear configurations of the reactants and products are adjusted to be the same without effectively transferring the electron. Therefore, the inner reorganization energy, $\lambda_{i,\mathrm{exch}}^{(\mathrm{I})}$ and $\lambda_{i,\mathrm{exch}}^{(\mathrm{II})}$, for the corresponding self-exchange reactions, can be estimated with eqn (8) and eqn (9) respectively. The two species participating during the first electron transfer process are the neutral compound ([Q]-PhNO$_2$: N) and the semiquinone as a radical anion ([Q$^{\bullet-}$]-PhNO$_2$: RA); meanwhile, at the second electron transfer process, they would be the semiquinone and the dianion biradical ([Q$^{\bullet-}$]-PhNO$_2^{\bullet-}$: DB) species electrogenerated from the reduction of the nitro group,

$$\lambda_{i,exch}^{I} = \begin{bmatrix} E(N\,as\,RA) \\ -E(N\,as\,N) \end{bmatrix} + \begin{bmatrix} E(RA\,as\,N) \\ -E(RA\,as\,RA) \end{bmatrix} \tag{8}$$

$$\lambda_{i,exch}^{II} = \begin{bmatrix} E(RA\,as\,DB) \\ -E(RA\,as\,RA) \end{bmatrix} + \begin{bmatrix} E(DB\,as\,RA) \\ -E(DB\,as\,DB) \end{bmatrix} \tag{9}$$

where E(X as Y) represents the energy of the species X within the optimized molecular structure of species Y. The required calculations were performed employing single point procedures for the optimized structures of [Q]-PhNO$_2$, [Q$^{\bullet-}$]-PhNO$_2$ and [Q$^{\bullet-}$]-PhNO$_2^{\bullet-}$ for compound **1**. In the case of a heterogeneous electron transfer process with only one reactant participating, the inner reorganization energy would be half the value calculated with eqn (8) and (9).

The calculated inner reorganization values with this procedure, employing the BLYP/TZVP method, for the first and second electron transfer processes were respectively 0.82 and 0.91 eV. These values are significantly higher than λ_o and they are indicative that changes in the nuclear configuration of the participating species are the determining factor in the $\lambda^{(\mathrm{I\ or\ II})}$ values obtained experimentally. Also, the higher $\lambda_{i,\mathrm{exch}}^{(\mathrm{II})}$ value can explain the quasi reversible voltammetric behavior of the second electron transfer process (signals IIc-IIa, Fig. 2) compared to the more reversible Ic-Ia couple (Fig. 2), bearing a lower $\lambda_{i,\mathrm{exch}}^{(\mathrm{I})}$ value. Therefore, electron self-exchange processes, as referred above to model inner reorganization, are useful to understand the observed experimental difference in λ values for both electron transfer steps.

The source of this higher inner reorganization component in relation to the total λ value was rationalized by comparing

‡ Another independent estimate for a_{Ox} was also obtained employing the calculated structures from quantum chemical procedures, from the volume of the solvated particle using a solvent probe radius for acetonitrile of 2.16 Å.[59] For the neutral and radical anion species, the respective radii determined were close to 7.07 Å for both. This result confirms that the molecule does not change its solvation radius significantly by modifying its charge and spin state, as commented on during the experimental analysis.

the structural differences between the participating species. The geometric parameters involving bond distances and angles (considering also dihedral angles), did not show a significant change between the calculated structures (see ESI†). However, the planes formed by the ring bearing the o-quinone moiety (C-2a · · · C-3a · · · C-4 · · · C-5 · · · C-5a · · · C-9a), with respect to the plane of the aromatic ring supporting the nitro function (C-1′ to C-6′), showed a shift in angle. A measure of this change in this angle was obtained from the improper torsion angle between bonds C-3a · · · C-4 and C-1′ · · · C-6′. This angle has a value of 139.6° in the neutral structure, almost the same value as for the semiquinone structure (139.4°). However, this angle changes within the biradical dianion structure, presenting a value of 132.6°. Considering the spin multiplicity and charge of the studied structures, this comparison indicates that more detailed electronic structure calculations are required to evaluate this change. However, the presented calculations allowed us to rationalize the structural modifications during electron uptakes. It should also be considered that such changes in torsion angles have already been addressed in discussing changes of λ for a series of nitro compounds,[61] although in that case, the most significant change occurs in the pyramidal structure of the nitro compound being reduced. This structural feature will be tested in a forthcoming work to determine the influence of these interactions on the electrochemistry of each reduced group, employing hydrogen-bonding schemes.

5. Conclusions

In this work, the electrochemical behaviour of an antitumoral nitroaromatic derivative obtained from nor-β-lapachone was studied. Cyclic voltammetric experiments, in acetonitrile solution, revealed that both quinone and nitro functions are reduced independently as *quasi*-reversible processes and afford different ion radical species. This fact was confirmed by performing *in situ* electrochemical-electron spin resonance (E-ESR) experiments, where the presence of a radical anion and a biradical dianion was established. The analysis of the kinetics of electron transfer associated to those electron uptake processes in terms of the Marcus–Hush–Levich model, revealed differences in the reorganization energy for both steps ($\lambda^{(I)}$: 1.07–1.11 eV; $\lambda^{(II)}$: 1.21–1.30 eV). By analyzing the conformations of the radical and biradical systems by calculations at the BLYP//TZVP level of theory, it was found that the inner component for the second reduction process ($\lambda_i^{(II)}$ was approximately 72% of $\lambda^{(II)}$), reflecting modifications in the nuclear structure during the radical anion–biradical dianion transition. This structural modification occurring during this electron uptake is also reflected in the differences presented by line widths of the ESR signals of both electrogenerated radical species and indicates that electron self-exchange processes have an important contribution to the stability of the electrogenerated biradical dianion. This result may explain the cytotoxicity of this dual-pharmacophoric compound. The generation of this dianion-diradical, in the presence of oxygen, is possibly related to an increase of oxidative burst that would be responsible for the oxidation of important endobiotics, causing disruption of redox homeostasis.[8] Studies along this line are under way and will be published elsewhere.

Acknowledgements

The authors thank Dr Alejandro Solano-Peralta and Dr Rafael Moreno Esparza (Facultad de Química, UNAM), for their help in the ESR spectrum acquisition. C. Frontana thanks CONACyT and SNI-Mexico for the grants and funding given for his postdoctoral studies. D. M. Hernández and D. P. Valencia thank CONACyT-Mexico for funding of their Ph. D. studies. The Brazilian agencies CNPq, CAPES, FAPEAL, Instituto do Milênio-Inovação em Fármacos/CNPq and FAPERJ are acknowledged for grants and fellowships.

References

1 M. N. da Silva, V. F. Ferreira and M. C. B. S. de Souza, *Quim. Nova*, 2003, **26**(3), 407.
2 C. Asche, *Mini-Rev. Med. Chem.*, 2005, **5**, 449.
3 P. J. O'Brien, *Chem.-Biol. Interact.*, 1991, **80**, 1.
4 T. J. Monks and D. C. Jones, *Curr. Drug Metab.*, 2002, **3**, 425.
5 T. J. Monks, P. Hanzlik, G. M. Cohen, D. Ross and D. G. Graham, *Toxicol. Appl. Pharmacol.*, 1992, **112**, 2.
6 J. L. Bolton, M. Trush, T. Penning, G. Dryhurst and T. J. Monks, *Chem. Res. Toxicol.*, 2000, **13**, 135.
7 F. C. de Abreu, P. A. M. Ferraz and M. O. F. Goulart, *J. Braz. Chem. Soc.*, 2002, **13**, 19 and references cited therein.
8 E. A. Hillard, F. C. de Abreu, D. C. M. Ferreira, G. Jaouen, M. O. F. Goulart and C. Amatore, *Chem. Commun.*, 2008, DOI: 10.1039/b718116g.
9 G. Roura-Perez, B. Quiroz, A. Aguilar-Martınez, C. Frontana, A. Solano, I. Gonzalez, J. A. Bautista-Martınez, J. Jimenez-Barbero and G. Cuevas, *J. Org. Chem.*, 2007, **72**, 1883.
10 M. Aguilar-Martínez, N. A. Macías-Ruvalcaba, J. A. Bautista-Martínez, M. Gómez, F. J. González and I. González, *Curr. Org. Chem.*, 2004, **8**, 1721.
11 J. A. Squella, S. Bollo and L. J. Núñez-Vergara, *Curr. Org. Chem.*, 2005, **9**, 565–581.
12 M. O. F. Goulart, A. A. De Souza, F. C. De Abreu, F. S. De Paula, E. M. Sales, W. P. Almeida, O. Buriez and C. Amatore, *J. Electrochem. Soc.*, 2007, **154**, P121.
13 T. K. Mukherjee, *J. Phys. Chem.*, 1967, **71**, 2277.
14 K. M. C. Davis, P. R. Hammond and M. E. Peover, *Trans. Faraday Soc.*, 1965, **61**, 1516.
15 E. S. Levin and Z. I. Fodiman, *J. Gen. Chem. USSR*, 1964, **34**, 1047.
16 A. I. Brodskii and L. L. Gordienko, *Theor. Exp. Chem.*, 1965, **1**, 2949.
17 A. E. Brodsky, L. L. Gordienko and L. S. Degtiavev, *Electrochim. Acta*, 1968, **13**, 1095.
18 P. W. Crawford, J. Gross, K. Lawson, C. C. Cheng, Q. Dong, D. F. Liu, Y. L. Luo, B. G. Szczepankiewicz and C. H. Heathcock, *J. Electrochem. Soc.*, 1997, **144**, 3710.
19 F. C. De Abreu, J. Tonholo, O. L. Bottecchia, C. L. Zani and M. O. F. Goulart, *J. Electroanal. Chem.*, 1999, **462**, 195.
20 E. N. da Silva Júnior, M. C. B. V. de Souza, A. V. Pinto, M. C. F. R. Pinto, M. O. F. Goulart, F. W. A. Barros, C. Pessoa, L. V. Costa-Lotufo, R. C. Montenegro, M. O. de Moraes and V. F. Ferreira, *Bioorg. Med. Chem.*, 2007, **15**, 7035.
21 M. O. F. Goulart, L. R. Freitas, J. Tonholo, F. C. de Abreu, D. S. Raslan, S. Starling, C. L. Zani, A. B. Oliveira and E. Chiari, *Bioorg. Med. Chem. Lett.*, 1997, **7**, 2043.
22 D. K. Roe , Overcoming solution resistance with stability and grace in potentiostatic circuits, in *Laboratory Techniques in Electroanalytical Chemistry*, ed. P. T. Kissinger and W. R. Heineman, Marcel Dekker, Inc., New York, USA, 1996.
23 P. He and L. R. Faulkner, *Anal. Chem.*, 1986, **58**, 517.
24 G. Gritzner and J. Kůta, *Pure Appl. Chem.*, 1984, **4**, 462.
25 deMon2k, A. M. Köster, P. Calaminici, M. E. Casida, R. Flores-Moreno, G. Geudtner, A. Goursot, T. Heine, A. Ipatov, F. Janetzko, J. M. del Campo, S. Patchkovskii, J. U. Reveles, D. R. Salahub and A. Vela, *deMon developers*, 2006.
26 A. Schaefer, H. Horn and R. Ahlrichs, *J. Chem. Phys.*, 1992, **97**, 2571.
27 A. Schaefer, C. Huber and R. Ahlrichs, *J. Chem. Phys.*, 1994, **100**, 5829.
28 C. Lee, W. Yang and R. G. Parr, *Phys. Rev.*, 1988, **37**, 785.

29 B. Miehlich, A. Savin, H. Stoll and H. Preuss, *Chem. Phys. Lett.*, 1989, **157**, 200.
30 J. E. Wertz and J. R. Bolton, *Electron Spin Resonance*, Chapman and Hall, New York, 1st edn, 1972.
31 N. A. Macías-Ruvalcaba, J. P. Telo and D. H. Evans, *J. Electroanal. Chem.*, 2007, **600**, 294.
32 M. E. Peover, *J. Chem. Soc.*, 1962, 4540.
33 A. Capon and R. Parsons, *J. Electroanal. Chem.*, 1973, **46**, 215.
34 J. Q. Chambers, Electrochemistry of quinones, in *The Chemistry of Quinonoid Compounds*, ed. S. Patai, John Wiley and Sons, New York, 1974, part 2, ch. 14.
35 A. H. Maki and D. H. Geske, *J. Am. Chem. Soc.*, 1961, **83**, 1852.
36 A. J. Fry, The electrochemistry of nitro, nitroso, and related compounds, in *The Chemistry of Amino, Nitroso, Nitro & Related Groups*, Supplement F2, ed. S. Patai, Wiley, New York, 1997, p. 837.
37 R. S. Nicholson, *Anal. Chem.*, 1965, **37**, 1351.
38 J. A. V. Butler, *Trans. Faraday Soc.*, 1924, **19**, 724–729.
39 T. Erdey-Grúz and M. Volmer, *Z. Physik. Chem.*, 1930, **150A**, 203.
40 R. A. Marcus, *J. Chem. Phys.*, 1956, **24**, 4966.
41 R. A. Marcus, *Electrochim. Acta*, 1968, **13**, 955.
42 N. S. Hush, *J. Chem. Phys.*, 1956, **28**, 952.
43 N. S. Hush, *Electrochim. Acta*, 1968, **13**, 1005.
44 C. Frontana and I. González, *J. Mex. Chem. Soc.*, 2008, **52**, 9.
45 M. Rudolph, *J. Electroanal. Chem.*, 2003, **543**, 23.
46 M. Rudolph, *J. Electroanal. Chem.*, 2004, **572**, 289.
47 M. Rudolph, *J. Electroanal. Chem.*, 2003, **558**, 171.
48 M. Rudolph, *J. Comput. Chem.*, 2005, **26**, 619.
49 M. Rudolph, *J. Comput. Chem.*, 2005, **26**, 633.
50 M. Rudolph, *J. Comput. Chem.*, 2005, **26**, 1193.
51 T. W. Rosanske and D. H. Evans, *J. Electroanal. Chem.*, 1976, **72**, 277.
52 R. A. Marcus, *J. Chem. Phys.*, 1955, **24**, 4955.
53 R. A. Marcus, *J. Chem. Phys.*, 1955, **43**, 579.
54 R. A. Marcus, *Electrochim. Acta*, 1958, **13**, 955.
55 M. J. Weaver, Redox reactions at metal–solution interfaces, in *Comprehensive Chemical Kinetics*, ed. Richard G. Compton, Elsevier, New York, 1987, vol. 27, ch. 1.
56 W. R. Fawcett, *Electrochim. Acta*, 1997, **42**, 833.
57 N. V. Rees, O. V. Klymenko, B. A. Coles and R. G. Compton, *J. Electroanal. Chem.*, 2002, **534**, 151.
58 N. Saha and B. Das, *J. Chem. Eng. Data*, 2000, **45**, 1125.
59 G. Osorio, C. Frontana, P. Guadarrama and B. Frontana-Uribe, *J. Phys. Org. Chem.*, 2004, **17**, 439.
60 S. F. Nelsen, S. C. Blackstock and Y. Kim, *J. Am. Chem. Soc.*, 1987, **109**, 677.
61 Ch. Kraiya, P. Singh and D. H. Evans, *J. Electroanal. Chem.*, 2004, **563**, 203.

